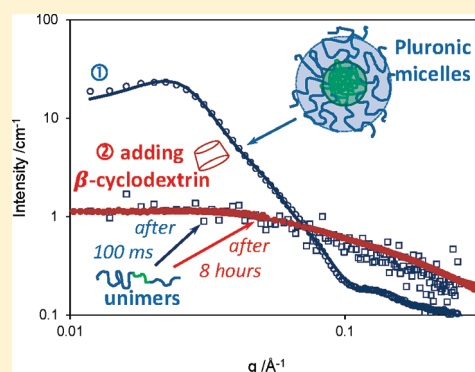


# Rupture of Pluronic Micelles by Di-Methylated $\beta$ -Cyclodextrin Is Not Due to Polypseudorotaxane Formation

Margarita Valero,<sup>†</sup> Isabelle Grillo,<sup>‡</sup> and Cécile A. Dreiss<sup>\*,§</sup><sup>†</sup>Departamento de Química Física, Facultad de Farmacia, Universidad de Salamanca, 37008 Salamanca, Spain<sup>‡</sup>Institut Laue-Langevin (ILL), DS/LSS, 6, rue Jules Horowitz, B.P. 156, 38042 Grenoble Cedex, France<sup>§</sup>Institute of Pharmaceutical Science, King's College London, Franklin-Wilkins Building, 150 Stamford Street, London SE1 9NH, United Kingdom Supporting Information

**ABSTRACT:** Spectroscopic measurements (uv/vis absorbance and fluorescence) and time-resolved small-angle neutron scattering experiments (TR-SANS) were used to follow the breakdown of Pluronic micelles by heptakis(2,6-di-O-methyl)- $\beta$ -cyclodextrin (DIMEB) over time in order to elucidate the mechanism of micellar rupture, generally attributed to polypseudorotaxane (PR) formation between the cyclodextrin and the central hydrophobic PPO block. The spectroscopic measurements with two different probes (methyl orange and nile red) suggest that very rapid changes (on the order of seconds) take place when mixing DIMEB with F127 Pluronic and that no displacement of the probe from the cyclodextrin cavity occurs, which is in disagreement with PR formation. TR-SANS measurements demonstrate for the first time that the micelles are broken down in less than 100 ms, which categorically rules out PR formation as the mechanism of rupture. In addition, the same mechanism is demonstrated with other Pluronics, P85 and P123. In the latter case, after micellar rupture, lamellar structures are seen to form over a longer period of time, thus suggesting that after the instantaneous micellar disruption, further, longer-scale rearrangements are not excluded.



## INTRODUCTION

Intricate supramolecular structures can be crafted and tuned through noncovalent interactions, leading to the design of smart materials with stimuli responsiveness, which are relevant to a range of technological fields. Cyclodextrins, cyclic oligosaccharides consisting of six, seven, or eight glucopyranose units ( $\alpha$ -,  $\beta$ -, and  $\gamma$ -CD), have been widely exploited to build up functional and responsive supramolecular structures.<sup>1–5</sup> Their toroidal shape and hydrophobic cavity give them the ability to form inclusion complexes (ICs) through noncovalent interactions with a variety of molecular guests that can fit into their cavity, including polymer chains,<sup>6</sup> forming so-called polypseudorotaxanes (PRs), where the CD is free to slide along the chain. Following the pioneering studies by Harada with poly(ethylene oxide) (PEO) and poly(propylene oxide) (PPO),<sup>6</sup> the formation of ICs with Pluronic triblock-copolymers, made up of a PPO central block flanked by two PEO blocks, has been reported.<sup>7–14</sup> We observed the disruption of Pluronic F127 micelles by heptakis(2,6-di-O-methyl)- $\beta$ -cyclodextrin (DIMEB structure available in the Supporting Information, Figure SI 1) using small-angle neutron scattering (SANS) measurements.<sup>15–17</sup> In contrast, micelles remained intact in the presence of the same amount of three closely related  $\beta$ -CD derivatives (structures available in the Supporting Information Figure SI 1), namely, heptakis(2,3,6-di-O-methyl)- $\beta$ -cyclodextrin (TRIMEB), 2-hydroxyethyl- $\beta$ -cyclodextrin (HEBCD), and

2-hydroxypropyl- $\beta$ -cyclodextrin (HPBCD).<sup>16</sup> We proposed<sup>15</sup> with others<sup>9,11,12</sup> that the cyclodextrin's macrocycle could thread onto PEO to localize preferentially on the hydrophobic middle group (PPO), therefore solubilizing it and reducing the driving force for micellization. However, the threading of  $\beta$ -CD along the PEO chain ( $\sim 100$  units), followed by its localization on the central PPO block, seems thermodynamically unfavored. Therefore, the possible establishment of nonspecific interactions between the cyclodextrin and the polymer, other than an inclusion complex, should be carefully considered in order to explain the dramatic increase in the cmc observed with DIMEB, as well as the remarkable and surprising sensitivity of this process to the nature of the  $\beta$ -CD substituents.<sup>16</sup> In a recent paper,<sup>18</sup> we revealed by nuclear magnetic resonance (NMR) the existence of weak interactions between the PPO methyl group and both the outer surface and cavity of the  $\beta$ -CDs but, surprisingly, no evidence of PR formation.

In this contribution, we use absorbance and fluorescence spectroscopy with two different probes and time-resolved SANS (TR-SANS) to bring more insight into the mechanisms of micellar rupture. The spectroscopic measurements suggest that structural changes occur very rapidly when mixing DIMEB with

Received: October 31, 2011

Revised: December 19, 2011

Published: December 21, 2011

Pluronic F127 (on the order of seconds) and that no displacement of the probe from the  $\beta$ -CD cavity occurs. These experiments were taken as an indication that the widely accepted PR model may not be valid under our conditions, and we therefore performed TR-SANS measurements in combination with a stopped-flow cell. Our results demonstrate for the first time that micellar rupture takes place in less than 100 ms, thus unambiguously ruling out the formation of a PR as a mechanism of rupture. Instead, micellar rupture must be attributed to an alternative type of association, based on weak interactions between the PPO groups and the methyl and hydroxyl groups of DIMEB, other than the widely invoked threading of  $\beta$ -CD along the polymer backbone. In addition, TR-SANS measurements on two alternative Pluronics, P85 and P123, are also presented.

## EXPERIMENTAL SECTION

**Materials.** Pluronic triblock copolymer F127 (average molecular weight ( $M_w$ ) of 12.6 kDa, PEO<sub>100</sub>PPO<sub>65</sub>PEO<sub>100</sub>), P123 ( $M_w$  5.8 kDa, PEO<sub>20</sub>PPO<sub>70</sub>PEO<sub>20</sub>), and P85 ( $M_w$  2.2 kDa, PEO<sub>25</sub>PPO<sub>40</sub>PEO<sub>25</sub>) were obtained from Sigma Aldrich, U.K. Heptakis(2,6-di-*O*-methyl)- $\beta$ -cyclodextrin, referred to as DIMEB (or  $\beta$ -CD or CD when there is no ambiguity), and hydroxypropyl- $\beta$  cyclodextrin (HPBCD) were obtained from Sigma Aldrich, U.K. The probes methyl orange, (MO,  $M_w$  327.3 g·mol<sup>-1</sup>) and nile red (NR,  $M_w$  318.4 g·mol<sup>-1</sup>) were purchased from Sigma Aldrich. All materials were used as received. D<sub>2</sub>O was purchased from Euriso-top with a purity of 99.85%.

**Preparation of the Solutions for Spectroscopic Measurements.** Solutions of the probes with either F127 or DIMEB were made by adding a small volume of concentrated solutions of MO ( $2.48 \times 10^{-3}$  M) to the appropriate amount of polymer or cyclodextrin and water to obtain final concentrations of  $2.48 \times 10^{-5}$  M MO, 10% F127, and 18% DIMEB. Appropriate volumes from a concentrated NR solution in ethanol ( $1.61 \times 10^{-4}$  M) were measured, and the solvent was evaporated. The residue was then solubilized in either water, 10% F127, or 18%  $\beta$ -CD (either DIMEB or HPBCD) aqueous solutions to achieve a final NR concentration of  $4.66 \times 10^{-6}$  M. Mixtures of 5% F127 and 9%  $\beta$ -CD were obtained by mixing equal amounts of 10% F127 or 18%  $\beta$ -CD (either DIMEB or HPBCD) and aqueous solutions of the probe.

Ternary solutions (F127/ $\beta$ -CD/probe) were made by mixing equal amounts of probe/10% F127 and probe/18%  $\beta$ -CD solutions, leading to concentrations of 5% F127, 9%  $\beta$ -CD, and an unchanged concentration of the probe ( $2.48 \times 10^{-5}$  M for MO and  $4.66 \times 10^{-6}$  M for NR).

**Fluorescence and Absorbance Spectroscopy Measurements.** Absorbance spectra were collected on a Perkin-Elmer Lambda 35 UV–vis spectrophotometer. Fluorescence emission measurements were performed on a Perkin-Elmer LS 50B spectrophotometer, with an excitation wavelength for NR of  $\lambda_{\text{exc}}$  = 540 nm.

The absorbance and emission spectra were deconvoluted in order to detect overlapped bands under the spectral contour and obtain the exact values of the maxima positions. For this purpose, the spectral envelope was assumed to be a sum of  $N$  Gaussian bands, whose intensity  $I(\nu)$  (for emission) is given by

$$I(\nu) = I(\nu_i) \exp \left[ -\ln 2 \left( \frac{(\nu - \nu_i)}{\delta_i} \right)^2 \right] \quad (1)$$

where  $I(\nu_i)$  is the emission intensity at  $\nu_i$ , the maximum position of the Gaussian band, and  $\delta_i$  is the width at half weight of the band. The same equation can be applied to the absorption bands, where the total absorbance intensity is  $A(\nu)$  and each Gaussian band is referred to as  $A(\nu_i)$ .

The binding constant of MO and NR to cyclodextrins,  $K_B$ , was determined by UV–vis absorbance and fluorescence spectroscopy. Assuming 1:1 inclusion complex formation, the measured intensity is related to the binding constant by the following expression<sup>19</sup>

$$I = \frac{(I_0 + I_\infty K_B [\text{CD}])}{1 + K_B [\text{CD}]} \quad (2)$$

where  $I$  is the measured absorbance or fluorescence intensity and  $I_0$  and  $I_\infty$  are the absorbance or fluorescence intensity when all of the probe is free and complexed, respectively (both are experimental parameters).  $[\text{CD}]$  is the concentration of free  $\beta$ -cyclodextrin, which corresponds to the experimental concentration because  $[\text{CD}] \gg [\text{probe}]$ .

This model was also used to determine the binding constant of both probes to the F127 micelles. In this case, the  $[\text{CD}]$  term is replaced by the micellar concentration,  $[M]$ , with  $[M] = ([\text{F127}] - \text{cmc})/N_{\text{agg}}$ . Values of  $N_{\text{agg}} = 50^{20}$  and  $\text{cmc} = 0.26\%$ <sup>21</sup> were used. For comparative purposes, the binding constant of NR to F127 was also determined by fitting the emission data to the model derived by Almgren<sup>22</sup>

$$\frac{(I_\infty - I_0)}{(I - I_0)} = (1 + K_{\text{eq}}[M])^{-1} \quad (3)$$

All solutions were prepared using Milli Q water, by weight, and % always refers to weight %.

**Time-Resolved Small-Angle Neutron Scattering Measurements (TR-SANS) Combined with the Stopped-Flow Technique.** The high flux of the spectrometers at the Institut Laue Langevin (Grenoble, France) enables real time measurements combined with the stopped-flow technique, with very short acquisitions of the order of 100 ms. The stopped-flow technique allows for rapid mixing of several solutions and triggers the reaction with the data acquisition, ensuring good reproducibility of the experiment.<sup>23</sup>

Kinetic SANS measurements were carried out on the D22 instrument at the ILL. The wavelength  $\lambda$  was set at 6 Å, the peak flux of the cold source. The sample-to-detector distance was 4 m, with a collimation at 5.6 m and a detector offset of 400 mm to maximize the available  $q$  range ( $1.2 \times 10^{-2} < q < 0.26 \text{ Å}^{-1}$ ). A  $7 \times 10 \text{ mm}^2$  sample aperture was used, and the sample path length in the Biologic SFM-300 stopped-flow apparatus was 1 mm.

Raw data were corrected for electronic background and empty cell and normalized by water using the new Lamp (Large Array Manipulation) ILL software developed for SANS data treatment ([http://www.ill.fr/data\\_treat/lamp/lamp.html](http://www.ill.fr/data_treat/lamp/lamp.html)).

The scattering measurements were made with an acquisition time for each frame  $n$  of  $t_n$  following a geometric series over 10 min

$$t_n = a^{n-1} t_1 \quad T_n = \frac{1 - a^n}{1 - a} t_1 \quad (4)$$

$T_n$  is the accumulated time after mixing, with  $t_1 = 100 \text{ ms}$  and  $a = 1.1$ . Sixty eight frames were measured for a total time of 651.7 s, after which 20 additional frames were measured with 1 s of exposure each.

The average time after mixing  $T_{AMn}$  for the  $n$ th run is

$$T_{AM1} = \frac{t_1}{2} + t_{DT} \quad \text{and} \quad T_{AMn} = \frac{T_{n-1} + T_n}{2} + t_{DT} \quad (5)$$

with  $t_{DT}$  as the dead time needed for filling of the cell estimated at 70 ms for the flow rate used (see below).

The stock solutions of Pluronic and  $\beta$ -CD were prepared by weighing the appropriate amounts of polymer,  $\beta$ -CD and deuterated water. Appropriate volumes of stock solutions (total of 804  $\mu$ L) were then mixed in the stopped-flow cell with a flow rate of 3 mL/s to obtain the target concentrations of 4–5 wt % Pluronic and 4–13 wt %  $\beta$ -CD.

Some of the samples used in the kinetic studies were measured after 1 month of rest on D11 (with  $\lambda = 10$  Å and detector distances of 8 and 1.2 m). Samples with P123 Pluronic and varying amounts of DIMEB at rest were measured on the LOQ instrument at the ISIS pulsed neutron source (ISIS, Rutherford-Appleton Laboratory, STFC, Didcot, Oxford).

**SANS Data Modeling.** Fits to the scattering curves of Pluronic micelles were performed using a form factor for block-copolymer micelles derived by Pedersen et al.<sup>24</sup> The micelles interact through a hard-sphere potential and coexist with their unimers. The total scattering intensity is expressed as

$$I(q) = \frac{c}{M} f F_{mic}(q) S(q) + \frac{c}{M_{uni}} (1-f) F_{uni}(q) \quad (4a)$$

where  $c$  is the polymer concentration (in w/v),  $M$  is the mass of a micelle,  $f$  is the weight fraction of the polymer included in the micelles,  $F_{mic}(q)$  is the micellar form factor,  $S(q)$  is the structure factor describing the intermicellar interactions at finite concentration,  $M_{uni}$  is the unimer mass, and  $F_{uni}(q)$  is the form factor of a unimer.

The model describes the micelles as having a compact spherical core of PPO, surrounded by dissolved chains of PEO, which obey Gaussian statistics. The form factor  $F_{mic}$  combines four different terms: the self-correlation of the sphere, the self-correlation of the chains, the cross-term between the sphere and chains, and the cross-term between the chains. Detailed expressions of the various form factors can be found in the original paper.<sup>24</sup>

The unimer's scattering form factor  $F_{uni}$  uses the Debye function<sup>25</sup>

$$F_{uni}(q) = \Delta\rho^2 \frac{(\exp(-x) - 1 + (x))}{x^2} \quad (5a)$$

where  $\Delta\rho^2$  is the total excess scattering length of the polymer with  $x = (qR_g^{uni})^2$  and  $R_g^{uni}$  as the radius of gyration of the unimers.

## RESULTS

**Absorbance and Fluorescence Spectroscopy.** In the first part of this work, we used two probes (MO and NR) to gain some insight into the time scale of micellar breakup and the formation or otherwise of a PR. In particular, it is expected that PR would induce a displacement of the probes from the CD cavity and would generate detectable structural changes over a long period of time because of the diffusion of both species and the threading of CD along the chains.<sup>26–28</sup>

**Absorbance Spectra with MO.** MO is a dye with a strong absorbance in the visible region of the spectrum, sensitive to the nature of the microenvironment in which it is present,<sup>29</sup> such as micelles and cyclodextrins.<sup>11,29</sup>

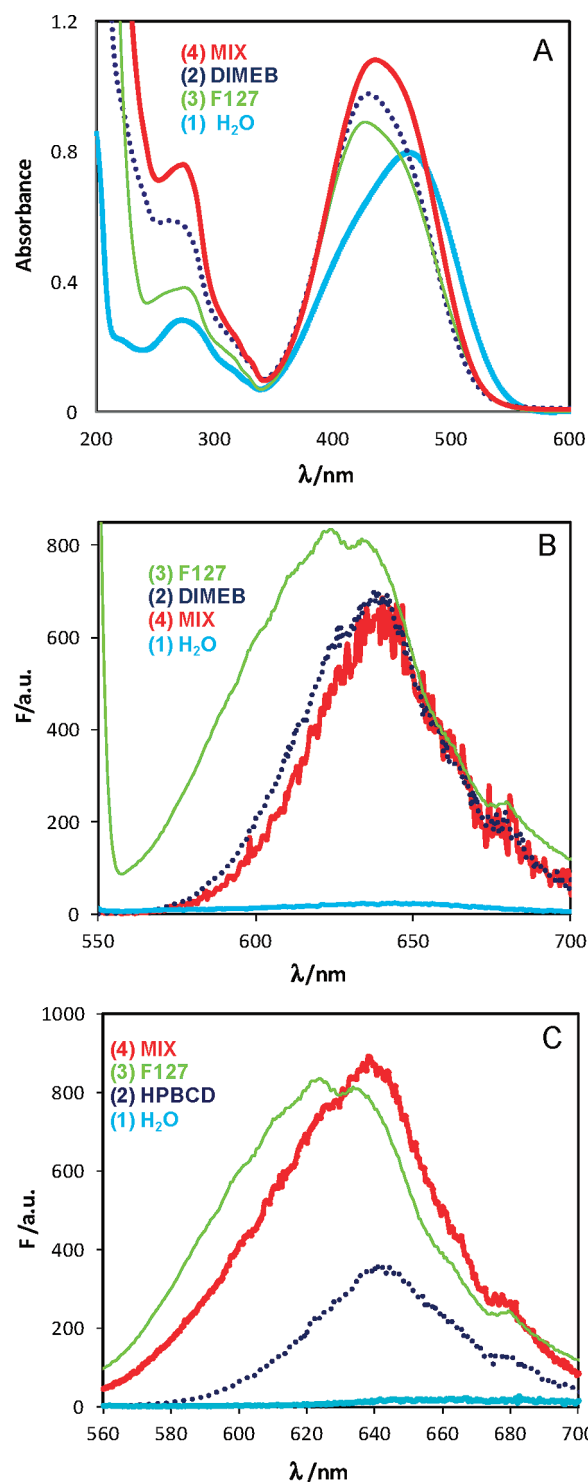


**Figure 1.** (A) Absorption spectra of MO ( $2.48 \times 10^{-5}$  M). (B) Fluorescence emission spectra of NR ( $4.66 \times 10^{-6}$  M). (C) Fluorescence emission spectra of NR ( $4.66 \times 10^{-6}$  M) in (1) H<sub>2</sub>O, (2)  $\beta$ -CD, (3) F127, and (4) mixtures of F127 and  $\beta$ -CD. In (A) and (B), the  $\beta$ -CD used is DIMEB; in (C), it is HPBCD. In each figure, the numbers from top to bottom correspond to the curves in order of decreasing intensity.

The absorbance spectra of MO in water, DIMEB, and F127 (Figure 1A, (1–3)) reveals a strong solvatochromism. In each case, the spectral contour of the main band can be fitted to a sum of two Gaussians (Supporting Information Figure S1 2).



**Table 1.** Deconvolution Parameters of the Absorption Spectra of MO and Fluorescence Emission Spectra of NR in Water, F127, DIMEB, and Mixtures of F127 and DIMEB<sup>a</sup>

MO/H <sub>2</sub> O			MO/DIMEB			MO/F127			MO/F127/DIMEB		
<i>A<sub>i</sub></i>	<i>ν<sub>i</sub></i>	<i>δ<sub>i</sub></i>	<i>A<sub>i</sub></i>	<i>ν<sub>i</sub></i>	<i>δ<sub>i</sub></i>	<i>A<sub>i</sub></i>	<i>ν<sub>i</sub></i>	<i>δ<sub>i</sub></i>	<i>A<sub>i</sub></i>	<i>ν<sub>i</sub></i>	<i>δ<sub>i</sub></i>
0.42	410	42	0.58	410	35	0.6	411	35	0.58	410	35
0.69	<b>472</b>	39	0.68	<b>456</b>	39	0.6	<b>460</b>	40	0.76	<b>457</b>	39
									0.08	472	39

NR/H <sub>2</sub> O			NR/DIMEB			NR/F127			NR/F127/DIMEB		
<i>F<sub>i</sub></i>	<i>ν<sub>i</sub></i>	<i>δ<sub>i</sub></i>	<i>F<sub>i</sub></i>	<i>ν<sub>i</sub></i>	<i>δ<sub>i</sub></i>	<i>F<sub>i</sub></i>	<i>ν<sub>i</sub></i>	<i>δ<sub>i</sub></i>	<i>F<sub>i</sub></i>	<i>ν<sub>i</sub></i>	<i>δ<sub>i</sub></i>
5.0	550	2	85	605	20	82	587	23	60	605	20
8.5	575	33	670	<b>638</b>	23	800	<b>626</b>	33	625	<b>639</b>	23
22.5	<b>645</b>	36	100	683	20	90	685	15	80	683	20

NR/HPBCD			NR/F127/HPBCD <sup>b</sup>			NR/F127/HPBCD <sup>b</sup>		
<i>F<sub>i</sub></i>	<i>ν<sub>i</sub></i>	<i>δ<sub>i</sub></i>	<i>F<sub>i</sub></i>	<i>ν<sub>i</sub></i>	<i>δ<sub>i</sub></i>	<i>F<sub>i</sub></i>	<i>ν<sub>i</sub></i>	<i>δ<sub>i</sub></i>
25	605	20	300	<b>615</b>	33	130	600	22
327	<b>642</b>	23	625	<b>640</b>	25	340	<b>627</b>	33
60	683	30	110	683	25	540	<b>642</b>	22
						115	683	20

<sup>a</sup> The maximum positions of the main band of each set of Gaussians are highlighted in bold. <sup>b</sup> The emission bands from NR in the mixture of F127 and HPBCD were deconvoluted both with three and four Gaussians (see text).

The proportion of each of these two bands changes with the environment (water, DIMEB, or Pluronic), and a clear shift in the position of the longer wavelength band is observed (Table 1): 472, 456, and 460 nm for H<sub>2</sub>O, DIMEB, and F127, respectively. These differences in the maximum absorbance of the probe warrant that the probe is sensitive enough to distinguish between the different environments (aqueous, cyclodextrin, and micelle interior).

Solutions of MO/F127 and MO/DIMEB were mixed in equal volumes, and the absorbance was measured immediately after mixing and followed over a long period of time (17 h). At these concentrations (5% F127/9% DIMEB), it is known from SANS experiments that the micelles are fully broken.<sup>17</sup> The absorbance spectrum of MO just after mixing (Figure 1A (4)) appears slightly shifted compared to that of F127 and DIMEB and with a higher absorbance, reflecting changes in the system. Over the 17 h of measurement, no further modification of the spectrum was observed; thus, the shift and the increase in absorbance reflect very rapid structural changes taking place between the mixing event and the first scan, which can be estimated to be ~45 s. The spectrum can be deconvoluted into three Gaussians (Table 1, Supporting Information Figure SI 2); two of them correspond to the absorbance maxima of MO in DIMEB and (a very small proportion of) MO in water. This clearly shows that upon mixing, MO is transferred from the interior of the micelles (because there is no peak at 460 nm) to the cyclodextrin's cavity and, importantly, that it does not leave the CD cavity over time.

The binding constants of MO to DIMEB and F127 were determined using UV–vis absorption spectroscopy. The data are well fitted to eq 2, giving binding constants of  $K = 2.8 \times 10^4$  and  $3.0 \times 10^3 \text{ M}^{-1}$  for DIMEB and F127, respectively. Therefore, the observed changes in the ternary system (MO/DIMEB/F127) could also be interpreted as a preferential location of the probe inside of the cyclodextrin and does not provide in

itself unambiguous evidence of micellar breakup nor does it strictly exclude PR formation.

**Emission Spectra with NR.** In order to clarify these results, NR was used as an additional probe. NR presents absorption and emission in the UV–vis region, sensitive to the polarity of its microenvironment, and has been used extensively as a probe for systems with restricted geometry, such as cyclodextrins and micelles.<sup>30</sup>

The emission spectra of NR in these systems differ markedly in intensity and maxima position (Figure 1B (1–3)). The emission spectra of the probe in water (Table 1, Supporting Information Figure SI 3) presents a broad band centered at 645 nm, lower than the reported value of 657 nm,<sup>31</sup> with a very low intensity, and in good agreement with the strong quenching produced by the intramolecular transfer charge state (ITC) in polar media.<sup>30</sup> A blue shift is observed when NR is in DIMEB (to 638 nm) and in F127 (to 626 nm) (Table 1), indicating a decrease in the polarity of the surroundings of the probe,<sup>30</sup> as well as a strong increase in the emission intensity. Therefore, the intensity and maximum position of the emission band enable a distinction between the three possible locations of the probe, H<sub>2</sub>O, F127 micelles, or DIMEB, thus validating the use of this probe for our purposes.

When mixing equal amounts of solutions containing either 10% F127 or 18% DIMEB, changes in the fluorescence occur instantaneously and are not modified further over the 45 min of the measurement, suggesting, as with MO, extremely rapid structural changes. The emission spectrum of NR in the mixture is very similar to the spectrum in pure DIMEB (Figure 1B (2) and (4)). The deconvolution (Table 1, Supporting Information Figure SI 3) clearly shows that the main band is centered at 639 nm, a very similar (slightly higher) position as that in the presence of DIMEB alone, confirming that NR interacts exclusively with DIMEB when the micelles are broken and that no

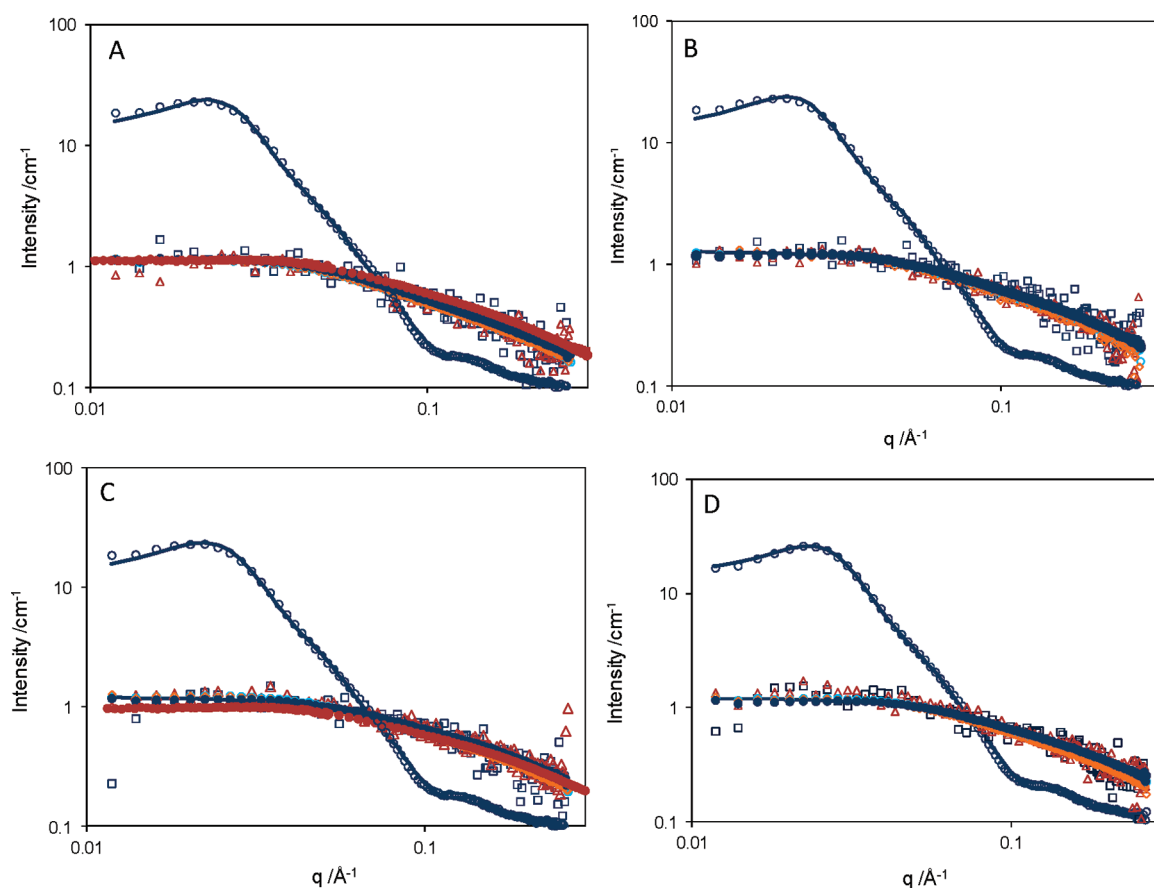


**Figure 2.** Small-angle neutron scattering data from Pluronic F127 micelles alone and in the presence of DIMEB, at different time points after mixing. (A–C) 4 wt % F127 micelles with 4.9 (A), 7.0 (B), and 8.6% (C) DIMEB. (D) 5% F127 with 7.6% DIMEB. For all graphs, the following plots are shown: F127 micelles (dark blue ○), and the mixtures after 0.1 (frame 1, dark blue □), 1.5 (frame 10, red △), 622.1 (frame 68, medium blue ○), and 642.1 s (frame 88, yellow ◇). The scattering from identical samples measured after 8 h (dark blue ●, A–D) and 1 month of rest (red ●, A, C) are also shown. Solid lines are fits to the block-copolymer micelles model and to the Debye model for Gaussian coils (see text for details).

displacement from the cyclodextrin by F127 (compatible with PR formation) is observed, in agreement with the experiments using MO as a probe.

As with MO, the binding constants of NR to DIMEB and F127 were obtained by fluorescence, giving  $K = 2 \times 10^4$  and  $10^5 \text{ M}^{-1}$ , respectively (the latter value was obtained with both eqs 2 and 3). These values show that, unlike MO, NR presents a higher affinity for F127 than DIMEB. Therefore, the changes observed in the probe emission must arise from the rupture of the micelles (already known for these systems<sup>17</sup>), not to a preferential localization in the cyclodextrin cavity. In order to confirm this result, we repeated the experiment with HPBCD (Figure 1C), which does not break the micelles.<sup>16</sup>

The deconvolution of the emission bands of NR (Table 1, Supporting Information Figure SI 4) shows the presence of a main band in the presence of HPBCD centered at 642 nm. Emission spectra were recorded at each minute after mixing NR/F127(10%) with NR/HPBCD (18%), for a total time of 35 min, over which period the spectrum remained unchanged. The deconvolution process shows that it is not possible to fit the spectrum from the mixture by exclusively using bands from NR/F127 and NR/HPBCD. The fit can be performed with three Gaussian bands (Table 1, Supporting Information Figure SI 4); the two most intense bands are centered at 640 nm (clearly corresponding to the NR/HPBCD complex) and 615 nm. This

second band is centered between the shorter wavelength band appearing in the binary systems, NR/F127 (587 nm) and NR/DIMEB (605 nm), and the most intense one appearing in F127 (626 nm); it is quite broad and with an important contribution. On this basis, a fit to four Gaussians was performed, which included all of the bands appearing in both binary systems (NR/HPBCD and NR/F127) (Supporting Information Figure SI 4). The fitting clearly demonstrates that part of the NR is in the cyclodextrins (642 nm band), but some is also inside of the micelle (627 nm band), in very good agreement with the co-existence of both systems. Considering the difference in the emission intensity of both Gaussians and the fact that the emission of NR is much more intense when inside of the micelles, it is clear that most probe molecules are still interacting with HPBCD.

The important points from these experiments are the following: (i) because NR has a higher affinity for F127 than for DIMEB or HPBCD, the shift of the probe from the micelle to the CD is not promoted and thus cannot be attributed to a preferential localization in the CD cavity; (ii) when F127 and HPBCD are present, an immediate change is observed and an equilibrium between the probe in the micelle and in the cyclodextrin is seen; therefore, the probe is immediately partitioned between the micelle and HPBCD; (iii) instead, when DIMEB and F127 are mixed, the probe is immediately displaced in totality to the CD cavity because the micelles are broken,

which confirms that breakup takes place immediately. These findings therefore lead to the following conclusions: F127 micelles break up very rapidly (on the order of seconds), and the largest proportion of the probe stays in the cavity of the cyclodextrins, which seems to contradict PR formation.

However, the amount of probe used is very low (compared to F127 and DIMEB concentrations); therefore, DIMEB could be involved in an inclusion complex with F127 and still be able to complex all probe present. In order to confirm that no shift of the probes from the DIMEB cavity is induced by F127, a competition experiment was performed.

The same probe concentration of either MO or NR was dissolved in 0.7% DIMEB, and increasing amounts of F127 were added up to 0.14%, which is below the cmc (0.26%<sup>21</sup>). Under these conditions, more than 95% of NR or MO is complexed (calculated from the binding constants quoted above). The CD concentration is much lower than that in previous experiments; hence, some shift of the complexed probe should be observed by adding a competing species. Moreover, the ratio CD/F127 is higher (0.7/0.14 versus 9/5 in the previous experiment), which should favor PR formation. In both cases, MO/DIMEB and NR/DIMEB, F127 addition did not produce any difference in the absorbance and emission spectra (data not shown). This thus confirms that the Pluronic is not able to displace the probes from the inner cavity of the cyclodextrin in monomeric or micellar form, which again seems to be in disagreement with the formation of a PR.

**Time-Resolved Small-Angle Neutron Scattering Experiments (TR-SANS).** Figure 2 presents the scattering results from a selection of solutions with 4 and 5 wt % F127 Pluronic micelles and in mixtures with varying amounts of DIMEB, immediately after mixing and over a period of  $\sim 10$  min. The scattering from the micelles alone was fitted with the core-shell copolymer micelle model derived by Pedersen and Gerstenberg.<sup>24</sup> The best fit was obtained with an aggregation number ( $N_{\text{agg}}$ ) of  $\sim 30$  and a solvent fraction in the core of 35% for 4 wt % F127 (Figure 2A–C), giving a core radius of  $\sim 4.1$  nm and a slightly higher aggregation at 5 wt % F127 ( $N_{\text{agg}} \approx 35$ ) with a lower solvent penetration of  $\sim 22\%$  (Figure 2D). The PEO shell thickness was found to be around 3.3 nm. For all samples shown in Figure 2, the first frame was taken immediately after mixing with the  $\beta$ -CD stock solution, with a delay time due to mixing that can be estimated to be  $\sim 70$  ms (cf. Experimental Section). In all cases, the scattering data immediately after mixing show an abrupt collapse of the intensity, with a loss of the characteristic features of a spherical form factor; this scattering pattern reflects the total rupture of the polymeric micelles, as observed previously.<sup>15–17</sup> The scattering intensity can be fitted to the Debye model for Gaussian coils,<sup>25</sup> giving a radius of gyration for all samples of  $\sim 16.5$  Å. The successive scattering curves (measured after 0.1, 1.5, 622.1, and 642.1 s) all superimpose perfectly; the better statistics at longer times are simply explained by the longer exposure times (cf. Experimental Section). Identical mixtures were also measured after resting for about 8 h (all samples) and 1 month (for samples shown in Figure 2A and C) and were also found to overlay perfectly, thus confirming that the structures formed immediately upon mixing are the final equilibrium states and that they are not modified over long periods of time (at least on the length scales probed by neutrons).

To assess the general validity of this result, two additional polymers were studied. Figure 3 shows the scattering from a smaller Pluronic, P85 (PEO<sub>25</sub>PPG<sub>40</sub>PEO<sub>25</sub>), before and after addition of 13% DIMEB. The scattering from 5 wt % micelles was

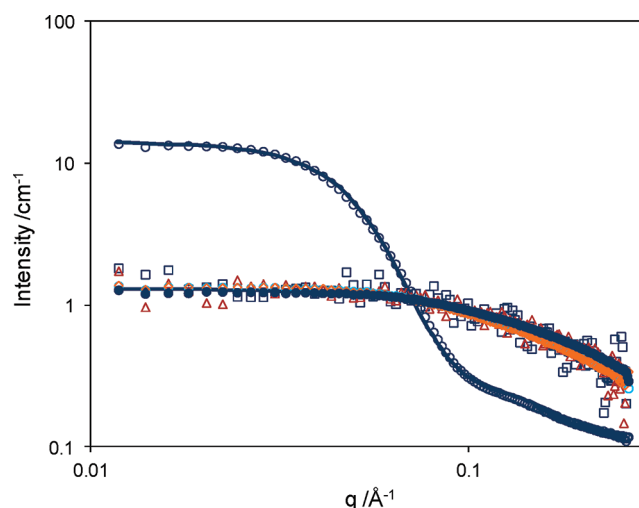


**Figure 3.** Small-angle neutron scattering data from 5 wt % Pluronic P85 micelles alone (dark blue  $\circ$ ) and in the presence of DIMEB at different time points after mixing: 0.1 s (frame 1, dark blue  $\square$ ), 1.5 s (frame 10, red  $\triangle$ ), 622.1 s (frame 68, medium blue  $\circ$ ), and 642.1 s (frame 88, yellow  $\diamond$ ) and after 8 h of rest (dark blue  $\bullet$ ). Solid lines are fits to the block-copolymer micelles model and to the Debye model for Gaussian coils (see text for details).

fitted with spheres of 4.7 nm core radius and  $\sim 40\%$  core hydration ( $N_{\text{agg}} \approx 44$ ). Right after mixing the polymer with DIMEB, a similar collapse of the intensity (as seen in Figure 2) is observed, confirming total, immediate rupture of the P85 micelles. A fit to the Debye model of Gaussian chains reveals coils of  $R_g \approx 11.5$  Å, in agreement with those of smaller P85 chains compared to F127.

Finally, we studied a Pluronic with an intermediate structure, P123, having 20 EO units on both sides (similar to P85) and 70 PO units as the central block (comparable to F127). This polymer is known to have a cloud point at around 93 °C and its solutions start to become cloudy at around 50 °C.<sup>32</sup> Figure 4A shows the scattering from 5 wt % P123 micelles with increasing amounts of DIMEB (5–13 wt %), which were measured about 1 month after preparation. The polymeric micelles are  $\sim 5.8$  nm in radius with  $N_{\text{agg}} \approx 100$ . At rest (Figure 4A), in the presence of increasing amounts of DIMEB, the intensity gradually decreases, and micellar features are smoothed out. At the highest  $\beta$ -CD concentrations studied (11 and 13 wt %), a sharp Bragg peak appears in the scattering, suggesting the presence of lamellar structures, which have been reported at higher concentrations of this polymer or in ternary systems with oil.<sup>33,34</sup> Figure 4B–D shows the time evolution of the intensity after mixing P123 micelles with 9.0, 10.7, and 13.2 wt %  $\beta$ -CD. As for F127 and P85 (Figures 2 and 3), a sharp drop of the intensity is observed in the first frame measured ( $\sim 100$  ms), and a partial loss of the typical features of spherical micelles is found, showing micellar disruption. We note however that the forward intensity increases a little over the  $\sim 35$  s of the measurements and is slightly higher still in the solutions that have rested for a few hours, suggesting the formation of larger structures or aggregates over time. With the highest concentration of  $\beta$ -CD studied (13.2%), this change over time is more drastic because a Bragg peak appears in the scattering after a long period of rest ( $\sim 8$  h), reflecting the formation of lamellar structures over time.<sup>33,34</sup> Therefore, although the addition of  $\beta$ -CD leads to sudden micellar disruption (faster than  $\sim 100$  ms), some structural rearrangements seem to be occurring over longer time scales. The final structures (in the presence of

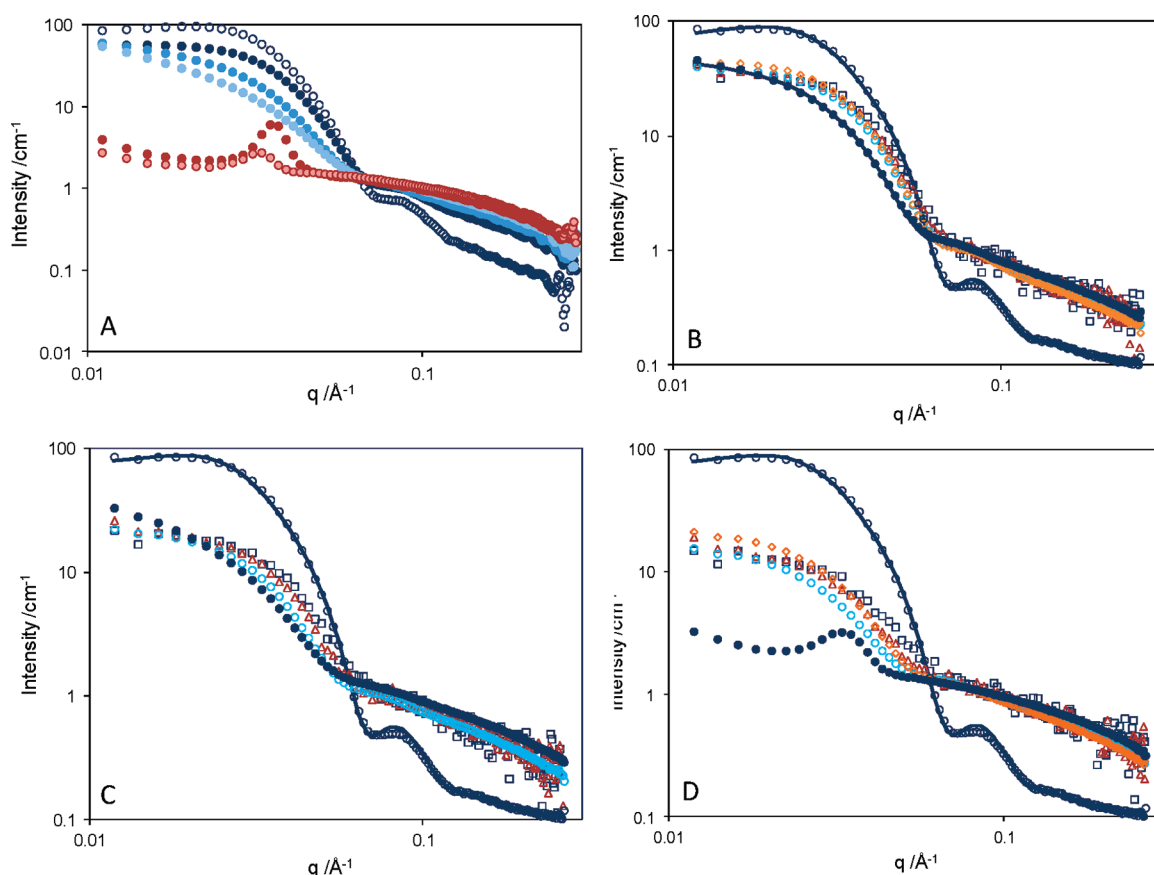


**Figure 4.** Small-angle neutron scattering data from 5 wt % Pluronic P123 micelles alone (dark blue  $\circ$ ) and (A) 1 month after preparation in the presence of DIMEB at different concentrations, 5 (dark blue  $\bullet$ ), 7 (medium blue  $\bullet$ ), 9 (light blue  $\bullet$ ), 11 (red  $\bullet$ ), and 13% (pink  $\bullet$ ), and at different time points after mixing with (B) 9.0, (C) 10.7, and (D) 13.2% DIMEB after 0.1 s (frame 1, dark blue  $\square$ ), 1.5 s (frame 10, red  $\triangle$ ), 622.1 s (frame 68, medium blue  $\circ$ ), and 642.1 s (frame 88, yellow  $\diamond$ ). The scattering from identical samples measured after 8 h (dark blue  $\bullet$ ) is also shown. Solid lines are fits to the block-copolymer micelles model (see text for details).

9.0 and 13.2%  $\beta$ -CD, Figure 4B and D) overlay perfectly with the signal from equivalent solutions measured 1 month after preparation (shown in Figure 4A); hence, these rearrangements must be occurring over a relatively short time scale, minor rearrangements on the order of seconds for 9.0 and 10.7%  $\beta$ -CD and possibly hours for the highest  $\beta$ -CD concentration studied of 13.2% (Figure 4D). In order to determine the nature of the structures formed in mixtures of P123 and DIMEB (below 11 wt %), a fit to the block-copolymer micellar model presented above was attempted; it is still able to describe the scattering of the solutions in the presence of 9.0 and 10.7 wt % DIMEB (solid line, Figure 4B), however with a strong reduction in micellized fraction (from  $\sim 90$  to 30%) and a higher level of hydration of the core. We do not exclude however the presence of a mixture of different structures, which prevents an unambiguous fit of the data. The position of the peak in the scattering (Figure 4A and D) gives lamellar spacings of approximately 180, 196, and 205 Å for 11 and 13 wt % DIMEB (Figure 4A) and 13.2 wt %  $\beta$ -CD (Figure 4D), respectively, larger than the values reported in ternary systems of P123 with oil.<sup>33,34</sup>

## DISCUSSION

The formation of PR is a kinetic process,<sup>26–28</sup> involving the diffusion of both partners (cyclodextrin and polymer), followed by the threading and sliding of CD molecules along the polymer backbone. Using spectroscopic experiments, based on the use of

a dye (MO) and a fluorescent probe (NR), we first demonstrated that the structural changes obtained by adding DIMEB to a solution of F127 are very rapid, while competitive experiments performed by “titrating” DIMEB solutions with F127 unimers suggested that F127 does not displace the probe from the interior of the cyclodextrin, which would have been expected in the case of PR formation. While these simple experiments are an indication that a mechanism other than the threading of  $\beta$ -CD along the polymer backbone may be the trigger of micellar rupture, they do not constitute a formal proof. The TR-SANS experiments, instead, demonstrate for the first time, and without ambiguity, that the structural changes leading to micellar breakup are instantaneous (less than  $\sim 100$  ms) and therefore completely rule out a mechanism based on PR formation. Instead, micellar rupture must be attributed to an alternative type of association, strong enough to overcome the hydrophobic drive of the aggregation, but other than the widely invoked  $\beta$ -CD threading. Our previous NMR measurements<sup>18</sup> had suggested the formation of a “loose” complex through weak interactions between the methyl group of the PPO block and the interior of the  $\beta$ -CD cavity. The absence of PR formation is also in better agreement with our previous observation<sup>16</sup> that this process is very discriminative; minor changes of the substituents on the  $\beta$ -CD rim (e.g., TRIMEB instead of DIMEB) are enough to prevent micellar rupture. Therefore, a very subtle balance of forces,



determined by the position and ratio of substituted and unsubstituted OH groups, is able to dictate the final structure and completely switch the behavior.

Our results also show that the instantaneous micellar disruption triggered by DIMEB can be generalized to other Pluronics than the previously studied F127;<sup>15–18</sup> however, the final structures depend on the exact PEO/PPO composition. While both F127 and P85 were immediately reduced to unimers, in P123 solutions, predominantly lamellar structures were found at high DIMEB to polymer ratios. The tendency to form bilayer structures is probably linked to the much lower HLB value of P123 (8 versus 22 for F127 and 16 for P85<sup>35</sup>).

We note also that, after the immediate micellar rupture (or disruption, in the case of P123), further time-dependent structural rearrangements are not excluded. Although they were only detected here with P123 as a small increase in the forward intensity (suggestive of further aggregation on large length scales) and, at the highest  $\beta$ -CD concentration studied, by the formation of lamellar aggregates, it is possible that larger-scale reorganization, outside of the range visible to neutrons, keeps occurring after the sudden breakup of the micelles. In fact, we do not rule out that, under specific conditions (concentration, CD/polymer ratio, etc), inclusion complexes are indeed formed once easier access to the polymer chains has been established by unimer formation, in agreement with other studies.<sup>11,12,36</sup> However, IC formation *cannot* be the cause of micellar breakup due to the extremely fast kinetics of the process revealed by these TR-SANS experiments. Slow time evolution of the structures has also been recently reported<sup>36</sup> and obtained by quenching of the samples below the CMT.

The exact nature of the interactions responsible for micellar breakup is difficult to pinpoint, but it is the subject of ongoing work, including molecular simulations and further NMR measurements. DIMEB is likely to hydrogen bond with PPO through its free hydroxyl group, therefore contributing to its solubilization. The finding that the trigger for these dramatic structural changes is not through IC formation has interesting implications; in particular, this suggests the possibility that micellar rupture could also be obtained with other molecules, provided that the correct balance of interactions is present. While CDs are increasingly used as the building blocks of responsive supramolecular structures through host–guest interactions,<sup>2,4,5</sup> in this particular case, the cavity of the cyclodextrins may not play any role in the drastic changes of self-assembly structures. These systems are of significant interest as smart and stimuli-responsive materials with tunable properties, in particular, for release applications.

## ■ ASSOCIATED CONTENT

**S Supporting Information.** Structure of the  $\beta$ -cyclodextrins described in this study (SI 1), deconvolution of the absorption spectra of methyl orange with water, F127, and DIMEB (SI 2), emission spectra of Nile Red with water, F127, and DIMEB (SI 3), and that with HPBCD (SI 4). This material is available free of charge via the Internet at <http://pubs.acs.org>.

## ■ ACKNOWLEDGMENT

The authors wish to acknowledge the ILL and ISIS for the provision of neutron beam time and Richard Heenan for help with the measurements at ISIS. Marcelo da Silva is thanked for

his contribution to the TR-SANS experiments. The model used to analyze the SANS data was kindly provided by Jan Skov Pedersen.

## ■ REFERENCES

- (1) Van de Manakker, F.; Vermonden, T.; Van Nostrum, C. F.; Hennink, W. E. *Biomacromolecules* **2009**, *10*, 3157–3175.
- (2) Yuen, F.; Tam, K. C. *Soft Matter* **2010**, *6*, 4613–4630.
- (3) Li, J.; Loh, X. J. *Adv. Drug Delivery Rev.* **2008**, *60*, 1000–1017.
- (4) Harada, A.; Takashima, Y.; Yamaguchi, H. *Chem. Soc. Rev.* **2009**, *38*, 875–882.
- (5) Du, L.; Liao, S. J.; Khatib, H. A.; Stoddart, J. F.; Zink, J. I. *J. Am. Chem. Soc.* **2009**, *131*, 15136–15142.
- (6) Harada, A.; Kamachi, M. *J. Chem. Soc., Chem. Commun.* **1990**, *19*, 1322–1323.
- (7) Topchieva, I. N.; Polyakov, V. A.; Kolomnikova, E. L.; Banatskaya; Kabanov, V. A. *Vysokomol. Soedin., Ser. A Ser. B* **1993**, *35*, A395–A398.
- (8) Panova, I. G.; Gerasimov, V. I.; Tashlitskii, V. N.; Topchieva, I. N.; Kabanov, V. A. *Polym. Sci., Ser. A* **1997**, *39*, 452–458.
- (9) Lazzara, G.; Milioto, S. *J. Phys. Chem. B* **2008**, *112*, 11887–11895.
- (10) Gaitano, G. G.; Brown, W.; Tardajos, G. *J. Phys. Chem. B* **1997**, *101*, 710–719.
- (11) Nogueiras-Nieto, N.; Álvarez-Lorenzo, C.; Sánchez-Macho, I.; Cocheiro, A.; Otero-Espinar, F. J. *J. Phys. Chem. B* **2009**, *113*, 2723–2782.
- (12) Tsai, C.-C.; Zhang, W.-B.; Wang, C.-L.; Van Horn, R. M.; Graham, M. J.; Huang, J.; Chen, Y.; Guo, M.; Cheng, S. Z. D. *J. Chem. Phys.* **2010**, *132*, 204903/1–204903/9.
- (13) Fujita, H.; Ooya, T.; Kurisawa, M.; Mori, H.; Terano, M.; Yui, N. *Macromol. Rapid Commun.* **1996**, *17*, S09–S15.
- (14) Fujita, H.; Ooya, T.; Yui, N. *Macromolecules* **1999**, *32*, 2534–2541.
- (15) Joseph, J.; Dreiss, C. A.; Cosgrove, T.; Pedersen, J. S. *Langmuir* **2007**, *23*, 460–466.
- (16) Dreiss, C. A.; Nwabunwanne, E.; Liu, R.; Brooks, N. J. *Soft Matter* **2009**, *5*, 1888–1896.
- (17) Valero, M.; Dreiss, C. A. *Langmuir* **2010**, *26*, 10561–10571.
- (18) Castiglione, F.; Valero, M.; Dreiss, C. A.; Mele, A. *J. Phys. Chem. B* **2011**, *115*, 9005–9013.
- (19) Nigam, S.; Durocher, G. *J. Phys. Chem.* **1996**, *100*, 7135–7142.
- (20) Prud'homme, R. K.; Wu, G.; Schneider, D. K. *Langmuir* **1996**, *11*, 4651–4659.
- (21) Sharma, P. K.; Reilly, M. J.; Jones, D. N.; Robinson, P. M.; Bhatia, S. R. *Colloids Surf. B* **2008**, *61*, 53–60.
- (22) Almgren, M.; Grieser, F.; Thomas, J. K. *J. Am. Chem. Soc.* **1979**, *101*, 279–291.
- (23) Grillo, I. *Curr. Opin. Colloid Interface Sci.* **2009**, *14*, 402–408.
- (24) Pedersen, J. S.; Gerstenberg, M. C. *Macromolecules* **1996**, *29*, 1363–1365.
- (25) Debye, P. *J. Phys. Colloid Chem.* **1947**, *51*, 18–32.
- (26) Ceccato, M.; Lo Nostro, P.; Baglioni, P. *Langmuir* **1997**, *13*, 2436–2439.
- (27) Lo Nostro, P.; Lopes, J. R.; Cardelli, C. *Langmuir* **2001**, *17*, 4610–4615.
- (28) Dreiss, C. A.; Newby, F. N.; Sabadini, E.; Cosgrove, T. *Langmuir* **2004**, *20*, 9124–9129.
- (29) Reeves, R. L.; Kaiser, R. S.; Maggio, M. S.; Sylvestre, E. A.; Lawton, W. H. *Can. J. Chem.* **1973**, *51*, 628–635.
- (30) Dutta, A. K.; Kamada, K.; Ohta, K. *J. Photochem. Photobiol., A* **1996**, *93*, 57–64.
- (31) Tajalli, H.; Ghanadzadeh Gilani, A.; Zakerhamidi, M. S.; Tajalli, P. *Dyes Pigm.* **2008**, *78*, 15–24.
- (32) Ganguly, R.; Kumbhakar, M.; Aswal, V. K. *J. Phys. Chem. B* **2009**, *113*, 9441–9446.
- (33) Holmqvist, P.; Alexandridis, P.; Lindman, B. *J. Phys. Chem. B* **1998**, *102*, 1149–1158.



- (34) Zipfel, J.; Berghausen, J.; Schmidt, G.; Lindner, P.; Alexandridis, P.; Richtering, W. *Macromolecules* **2002**, *35*, 4064–4074.
- (35) Kozlov, M. Y.; Melik-Nubarov, N. S.; Batrakova, E. V.; Kabanov, A. V. *Macromolecules* **2000**, *33*, 3305–3313.
- (36) Perry, P.; Hébraud, P.; Gernigon, V.; Brochon, C.; Lapp, A.; Lindner, P.; Schlatter, G. *Soft Matter* **2011**, *7*, 3502–3512.